International Journal of Power Electronics and Drive Systems (IJPEDS)
Vol. 13, No. 3, September 2022, pp. 1684~1695
ISSN: 2088-8694, DOI: 10.11591/ijpeds.v13.i3.pp1684-1695

Wind energy management of a standalone system operating at maximum power point

Hani Albalawi[1,2], Sherif A. Zaid[1,2], Yonis M. Buswig[3], Hassan Wedaa El-Rab[1], Abderrahim Lakhouit[4], Muhammed Ayas Arshad[5]
[1]Department of Electrical Engineering, Faculty of Engineering, University of Tabuk, Tabuk, Saudi Arabia
[2]Renewable Energy and Energy Efficiency Centre (REEEC), University of Tabuk, Tabuk, Saudi Arabia
[3]Department of Electrical and Electronic Engineering, Faculty of Engineering, Universiti Malaysia Sarawak, Samarahan, Malaysia
[4]Department of Civil Engineering, Faculty of Engineering, University of Tabuk, Tabruk, Saudi Arabia
[5]Sensor Networks and Cellular System Research Centre, University of Tabuk, Tabruk, Saudi Arabia

Article Info

Article history:

Received Mar 19, 2022
Revised Jun 7, 2022
Accepted Jun 22, 2022

Keywords:

Energy storage
Maximum power point
Standalone
Wind energy

ABSTRACT

In this paper, the management and control of a standalone wind energy system versus variations of wind speed and load are investigated. The system includes a wind turbine coupled to a variable-speed permanent magnet synchronous generator (PMSG), rectifier, boost converter, power inverter, and an energy storage system (ESS). The ESS is a very important part to achieve system stability and support the maximum power point tracking (MPPT) operation. A simple off-line MPPT algorithm is introduced that can be accomplished using the boost converter. The system dynamic model is derived then the control and energy management algorithms are introduced to improve the system performance. The MATLAB platform has been utilized to simulate the proposed system under different disturbances in the load power and wind speed. The results show perfect management of the system energy, good performance of the DC link voltage, stable load voltage, and load frequency.

Corresponding Author:

Sherif A. Zaid
Department of Electrical Engineering, Faculty of Engineering, University of Tabuk
Tabuk 71491, Saudi Arabia
Email: shfaraj@ut.edu.sa

1. INTRODUCTION

Nowadays, standalone energy generation systems are becoming widespread in islands and rural regions. The reason behind this is the grid is usually not available due to economic issues. Commonly, diesel generators are utilized for electricity production in remote area applications. Though these generators have high reliability, simple starting, and low installation cost, it requires regular maintenance, high running cost, and has bad environmental impacts [1]. Standalone wind systems incorporating an energy storage system provide a good alternative to classical diesel generators. It is environmentally friendly and has no running cost [2].

As wind power is intermittent in nature, it can not supply steady electrical power to loads. To overcome this problem, an energy storage device can be employed in order to store/supply energy in such a way as to compensate for the wind energy variations significantly. Therefore, energy storage systems are essential for the stability and reliability of wind energy system operation [3]-[10]. Also, it supports the transient stability of the system against load and wind fluctuations [11]. Different kinds of energy storage systems have been utilized like batteries, flywheels, superconducting magnetic energy storage (SMES), supercapacitors, hydrogen, thermal, and compressed air energy storage. However, lead-acid batteries are the common energy storage for many applications due to their merits of low cost, wide operating temperature, and high cell voltage [12]. Therefore, the lead-acid batteries strongly support the development of standalone wind systems [13].

For any wind energy system, there are two main components, which are the electrical generator and the mechanical wind turbine. Many types of generators have been implemented in the wind systems such as the permanent magnet synchronous generator (PMSG) and the induction generator [14], [15]. Nevertheless, PMSGs are suitable for low power wind systems as it has high energy density, self-excitation, and compact size. It can be used to generate power from gearless wind turbines [16].

The annual generated energy of standalone wind systems could be increased by applying maximum power point tracking (MPPT) must for variable-speed wind systems [17]. Various maximum power point tracking MPPT techniques have been proposed. Such techniques can be classified into; i) the hill-climbing search technique, ii) the power signal feedback technique [18], iii) the quasi-MPPT control technique [19], and iv) fuzzy logic control technique [20].

Recently, there are much research in the area of the analysis, design, control, and modeling of standalone wind energy systems [21]-[24]. Musarrat *et al.* [21] introduces a PMSG-based wind power system with an ESS utilizing an SMES with high-temperature. However, the system was complex and expensive. A common-mode voltage suppression for a standalone wind power conversion system utilizing PMSG is introduced by [22]. The proposed system has not considered the MPPT and the system efficiency is low. Hui *et al*. [23] provides an energy management algorithm with adaptive MPPT and power limit capability. However, the study was suitable for small standalone systems. Another MPPT scheme for standalone wind systems has been introduced in [24].

The problem of this research is addressing the energy management of a standalone wind system incorporating an energy storage system. Also, a new off-line MPPT algorithm is proposed to maximize the delivered energy from the wind turbine. The technique is very simple and uses the wind turbine characteristics curves to generate the gate pulses for a boost converter that is cascaded to the rectifier terminals for this purpose. Hence, the boost converter function is to solve the MPPT problem of the proposed system. The proposed system includes the wind turbine, PMSG generator, rectifier, boost converter, energy storage system, bidirectional charger, and power inverter. Compensation of high-frequencies harmonics is attained by employing a simple filter. The system has four controllers used to manage the system energy, implement MPPT, regulate the charge/discharge process of the storage battery, control the voltage of the DC link, control the inverter frequency and voltage. The controllers' main objective is to alleviate the intermittence problem of wind energy and regulate the storage of excess energy. The proposed system has been simulated using MATLAB/Simulink platform. The system is tested under several step changes in the wind speed and load power. The results show good performance and energy management under all disturbances. The manuscript is arranged as follows: Section 2 introduces the configuration and modeling of the introduced system. In section 3 the proposed system controllers are presented. The discussion of the system simulation results are proposed in section 4. Finally, section 5 provides the paper net conclusions.

2. THE CONFIGURATION AND MODELLING OF THE INTRODUCED SYSTEM

This section introduces the configuration, analysis, and modeling of the proposed system. The introduced isolated wind power system is illustrated in Figure 1. The system includes a variable speed wind turbine, that is coupled to a PMSG. The PMSG is connected to an uncontrolled rectifier with a filter. The output of the filter is connected to a boost converter to help in supporting the MPPT state. The output of the boost converter constitutes the system DC-link. It is connected to both the power inverter and the bidirectional charging converter. The charging converter regulates the DC bus voltage and controls the charging-discharging processes of the storage battery. On the other hand, the inverter supplies the isolated load with a regulated voltage and frequency. The model of the whole proposed wind system is carried out in the following subsections.

2.1. Wind turbine model

The wind turbine dynamic characteristics are specified in terms of the power coefficient (C_p) which is a function of the blade pitch angle (β) and the tip speed ratio (λ). The optimum value of λ should be used to have the best utilization the wind energy. Therefore, the corresponding C_p will be supreme. The wind turbine power coefficient and tip speed ratio are expressed as (1) [24]:

$$\lambda = \frac{\omega_m R}{v_w} \tag{1}$$

$$C_p(\lambda, \beta) = (0.44 - 0.0167\beta)\sin(\pi(\lambda - 3)/(15 - 0.3\beta)) - 0.00184(\lambda - 3)\beta \tag{2}$$

Where (R) is the rotor radius of the turbine, (ω_m) is the angular mechanical speed of the rotor, and (v_w) is the wind speed of the turbine. The turbine output power (P_m), may be given by (3) [24].

$$P_m = A\rho v_w^3 C_p(\lambda, \beta)/2 \tag{3}$$

Where (ρ) is the air density and (A) is the blades swept area.

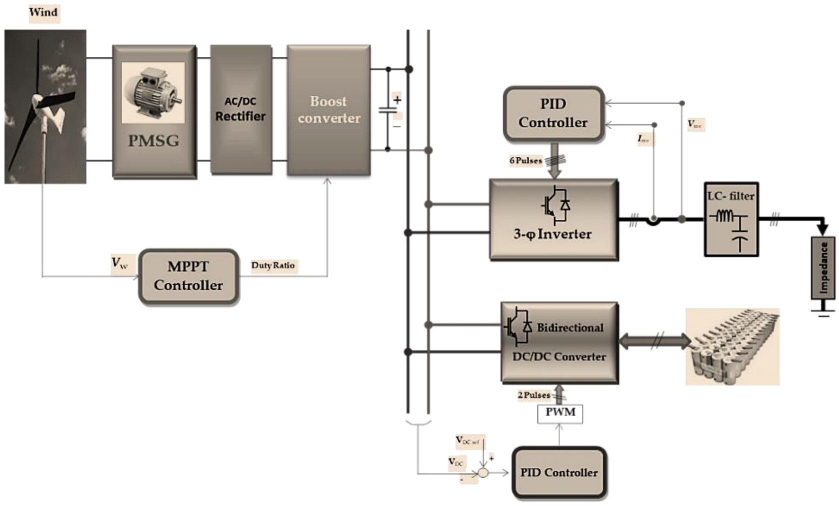

Figure 1. The proposed isolated wind energy system

2.2. PMSG model rectifier model

The PMSG generator has the dynamic model, in the d–q rotor frame, given by [23]:

$$\frac{di_{sd}}{dt} = (-i_{sd}r_s + pi_{sq}\omega_m L_q - V_{sd})/L_d \tag{4}$$

$$\frac{di_{sq}}{dt} = (-i_{sq}r_s + p\omega_m(i_{sd}L_d + \lambda_m) - V_{sq})/L_q \tag{5}$$

Where (r_s) is the stator resistance, (i_{sq}) is the stator-current quadrature-component, (i_{sd}) is the direct component of the stator current, (L_d, L_q) are the stator d- and q-axis inductances. (p) is the pole pairs, (λ_m) is the permanent flux linkage. The mechanical dynamics are given by (6).

$$\frac{d\omega_m}{dt} = (\frac{P_m}{\omega_m} - 1.5p\lambda_m i_{sq})/J \tag{6}$$

Where (J) is the moving parts inertia.

2.3. Rectifier model

The PMSG speed is direct related to the wind turbine speed and affected by its variations. Hence, the generator output voltage and frequency vary. This issue is not acceptable for the system loads. To alleviate this problem, the PMSG output is transformed to DC voltage and thereafter reconverted to AC voltage has the required frequency and amplitude. An uncontrolled 3-φ rectifier is utilized for this purpose. Assuming that the effect of source inductance is neglected, the rectifier average output voltage and current (V_{dc} , I_{dc}) is represented by (7) [24].

$$V_{dc} = 1.654V_h \, , I_{dc} = 0.907I_h \tag{7}$$

Where; (V_h , I_h) are the PMSG rms phase voltage and current.

2.4. Boost converter model

Figure 2 demonstrates the boost converter circuit diagram. Its input is the uncontrolled rectifier output however its output constitutes the system DC bus. Its task is to control the PMSG power to act at the MPPT state. The converter dynamic model is given by [25]:

$$V_p = L_{bb}\frac{dI_p}{dt},\ Q_b \rightarrow on \tag{8}$$

$$V_p - V_{dc} = L_{bb}\frac{dI_p}{dt}, Q_b \rightarrow off \tag{9}$$

where (V_{dc}) is the DC link voltage and (L_{bb}) is the converter inductance.

2.5. Battery storage system model

The ESS includes a bidirectional converter and a lead-acid battery bank. Its function is to store the spare wind energy greater than the load demand. Then use this storage to recover for the decrease in the wind energy at low generated periods. The battery model or equivalent circuit includes a voltage-controlled voltage source in series with internal resistance.

2.6. Bidirectional charge converter model

The function of this converter is managing the discharge/charge processes of the ESS. It can supply power through the two directions. The circuit construction of this converter is presented in Figure 3. The input terminals of this converter are attached to the system DC link. Nevertheless, its output terminals are connected to the storage battery. The operation of this converter may be classified into two modes called the buck mode and boost mode. The converter acts in the step-down mode if the switch S_2 is off and the switch S_1 is modulated. At this mode, the storage battery is charging. However, it acts in the step-up mode if switch S_1 is off and the switch S_2 is modulated. At this mode, the storage battery is discharging.

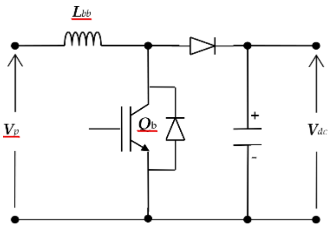

Figure 2. Boost converter circuit

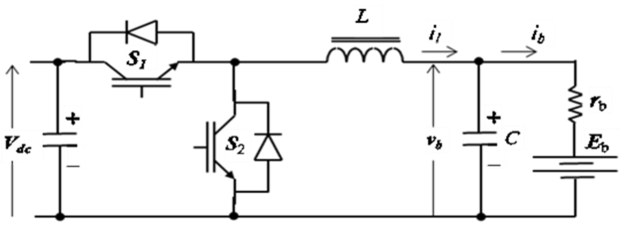

Figure 3. The ESS bidirectional-converter circuit

The model of the circuit is described by:

- The buck (charge) mode:

$$\dot{\boldsymbol{X}} = \begin{bmatrix} 0 & \frac{-1}{L} \\ \frac{1}{C} & \frac{-1}{r_b C} \end{bmatrix}\boldsymbol{X} + \begin{bmatrix} \frac{V_{dc}}{L} \\ 0 \end{bmatrix} S_1 + \begin{bmatrix} 0 \\ \frac{E_b}{r_b C} \end{bmatrix} \tag{10}$$

$$\boldsymbol{X} = \begin{bmatrix} i_l \\ v_b \end{bmatrix} \tag{11}$$

Where (E_b, r_b) are the voltage of the storage battery and the internal resistance, (v_b, i_l) are the capacitor voltage and inductor current, S_1 is a binary number representing the switching state [0,1], (V_{dc}) is the voltage of the DC bus, (C) is the filter capacitance, and (L) is the filter inductance.

- The boost (discharge) mode:

$$\dot{\boldsymbol{X}} = \begin{bmatrix} 0 & \frac{-1}{L} \\ \frac{1}{C} & \frac{-1}{C r_b} \end{bmatrix}\boldsymbol{X} + \begin{bmatrix} \frac{-V_d}{L} \\ 0 \end{bmatrix} Q_2 + \begin{bmatrix} \frac{V_{dc}}{L} \\ \frac{E_b}{C r_b} \end{bmatrix} \tag{12}$$

Where S_2 binary number represents the switching state of S_2 [0,1].

2.7. Inverter model

The 3-φ inverter circuit including a filter is presented in Figure 4(a). For modeling purposes, the space vector representation of the inverter 3-φ quantities is important. Hence, all currents and voltages of the inverter are represented using:

$$\underline{A} = 2/3(v_a + \propto v_b + \propto^2 v_c) \tag{13}$$

Where; (v_a, v_b, and v_c) are the actual 3-φ values, $\underline{A}$ is the equivalent space vector, and $\propto = e^{j(2\pi/3)}$. The 3-φ two-level inverter has eight switching states which may be transferred to, according to (13), space vectors presented in Figure 4(b). The inverter dynamic model can be represented as:

$$\dot{Z} = \begin{bmatrix} 0 & \frac{-1}{L_f} \\ \frac{1}{C_f} & 0 \end{bmatrix} \boldsymbol{Z} + \begin{bmatrix} V_{dc}/L_f \\ 0 \end{bmatrix} \underline{S} - \begin{bmatrix} 0 \\ \underline{I}_o/C_f \end{bmatrix} \tag{14}$$

$$Z = \begin{bmatrix} \underline{I}_f \\ \underline{V}_c \end{bmatrix} \tag{15}$$

where (C_f, L_f) is the filter capacitance and filter inductance, ($\underline{I}_o$) is the space vector of the output current, ($\underline{S}$) is the switching states space vector, ($\underline{V}_c$) is the capacitor voltage space vector, and ($\underline{I}_f$) is and the space vector of the filter current.

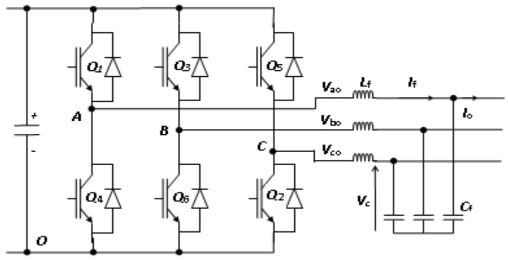

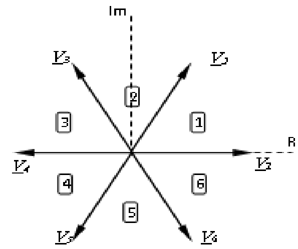

(a) (b)

Figure 4. The 3-φ inverter (a) circuit diagram and (b) possible voltage space vectors

3. THE PROPOSED SYSTEM CONTROLLERS

This section proposes the details of the system controllers, the boost converter controller, MPPT controller, and inverter controller. A simple MPPT algorithm is proposed to extract maximum power from the wind turbine. The proposed system has three main controllers the load inverter controller, the bidirectional controller, and the MPPT controller. The following subsections discuss those controllers in detail.

3.1. Load inverter controller

The load inverter is a two-level 3-φ voltage source inverter. It is a current-controlled inverter. It has two nested control loops, as displayed in Figure 5(a), which are used to control the inverter. The output voltage is controlled via the outer loop. The error signal produced by comparing the actual output voltage with the reference value is fed to a PI controller that produces the required reference current for the inner loop. Hence, it is compared to the actual current and fed to a PWM modulator to get the converter transistors' signals.

3.2. Charge converter controller

The chare converter controller controls the charge/discharge processes of the energy storage system. Also, it controls the system DC link voltage. Hence, a simple PID controller is used for this issue as shown in Figure 5(b). The control system has two nested controllers. The first one is used for controlling the current, However, the loop outer is used for controlling the voltage. This method is called the constant voltage-current method. The PID parameters are tuned using the Ziegler–Nichols tunning technique.

3.3. MPPT controller

In wind power systems, the principle of MPPT is to maximize the power output by optimizing the speed of the PMSG concerning the wind velocity. Numerous researchers have been done to get better performance MPPT for wind systems [26], [27]. A simple and new MPPT algorithm has been introduced. It uses the wind turbine characteristics curves to find a mathematical model of the MPPT controller. The MPPT in this paper is based on the characteristic curves of the wind turbine. The datasheet for the wind turbine is used to generate the P_m-ω_m curves for different wind speeds as presented in Figure 5(c). Also, the controller is shown in Figure 5(c). The input for this controller is the wind speed (V_w) however, its output is the boost converter duty ratio (k). For the MPPT operation, it is assumed that the boost converter input current is continuous, the voltage gain is:

$$\frac{V_{dc}}{V_r} = \frac{1}{1-k} \quad (16)$$

To operate the wind turbine at the MPPT state, the rectifier terminal voltage should be at a peak voltage condition (V_{rm}). The duty cycle at MPPT conditions (k_{mpp}) is given by:

$$k_{mpp} = 1 - \frac{V_{rm}}{V_{dc}} \quad (17)$$

The value of V_{rm} is calculated using the wind turbine curves for a given wind speed. Hence, the duty cycle and the wind velocity relation can be generated as:

$$k_{mpp} = 2.055e^{-5}v_w^4 - 1.191e^{-3}v_w^3 + 0{,}02212v_w^2 - 0.2359v_w + 1.564 \quad (18)$$

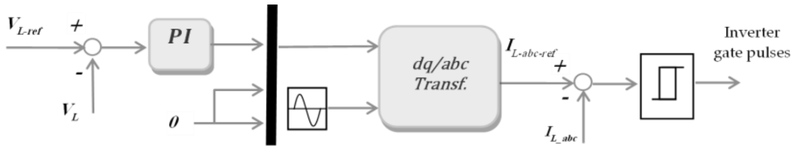

(a)

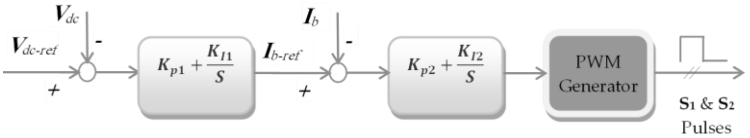

(b)

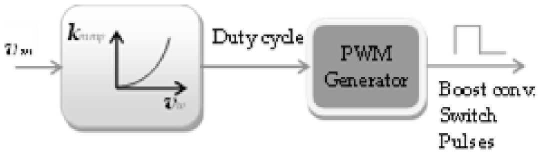

(c)

Figure 5. The proposed system controllers block diagrams, (a) load inverter controller, (b) bidirectional converter controller, and (c) the MPPT controller

4. SIMULATION RESULTS

In this section, the evaluation of the proposed system responses are carried out by discussing the digital simulation results. The parameters of the proposed system are shown in Table 1. The simulations have been carried out using the MATLAB/Simulink platform. Figure 6 (see Appendix) provides the results for different variables of the proposed standalone wind system. Forced step changes in the wind velocity are applied as shown in Figure 6(a). It is noticed rotating speed of the PMSG changes with the wind velocity, as shown in Figure 6(b). However, it has relatively long transient times due to the high inertia of the rotating parts. The PMSG torque response is shown in Figure 6(c). The deriving torque of the shaft must be kept within a safe limit to avoid destruction. In Figure 6(d), the DC-link voltage is remained stable and tracks well its reference value. Small overshoots, less than 2%, have occurred indicating good performance. The charging current of the ESS is demonstrated in Figure 6(e). The figure indicates the charging current of the ESS battery during the high wind energy periods, $0 < t < 1.35$s. Also, the charging current level increases with the wind energy increase. On the other hand, the current reverses its direction, discharge mode, when the wind energy cannot generate all the required power at low wind velocities.

The system powers are shown in Figure 6(f); the turbine power, the ESS power, and the output power. At the charging periods, the sum of the output power and the ESS power is less than the turbine power by some losses. The ESS power is positive at these periods. Nevertheless, at the discharging periods, the ESS changes to negative and added to the wind energy to supply the load.

The load 3-φ voltages, shown in Figure 6(g), are sinusoidal with constant amplitude and frequency for all load and wind velocity disturbances. Figure 6(h) shows the 3-φ load currents. It is sinusoidal with constant frequency, 50Hz, and variable amplitude related to the load power demand. The currents are in phase with the grid voltage, as the load has a unity power factor.

The load current THD is 1.28% at a wind velocity of 12 m/s. However, it varies with different variables and dominantly with wind velocity, as demonstrated in Figure 7(a). Figure 7(b) presents the alteration of the load current frequency spectrum @ wind velocity of 12 m/s. The figure indicates that lower-order harmonics of the load current are very small and the THD is low. The dominant harmonic is the 13th harmonic which has an amplitude of 0.95%.

Table 1. System parameters

Parameter	Value
Power rating of the wind turbine	10 KW
V_{DC}	300 V
C	3300 μF
PWM switching frequency	10 KHz
Load voltage	110 V
Load frequency	50 Hz
L_f	0.003 H
C_f	2 μF

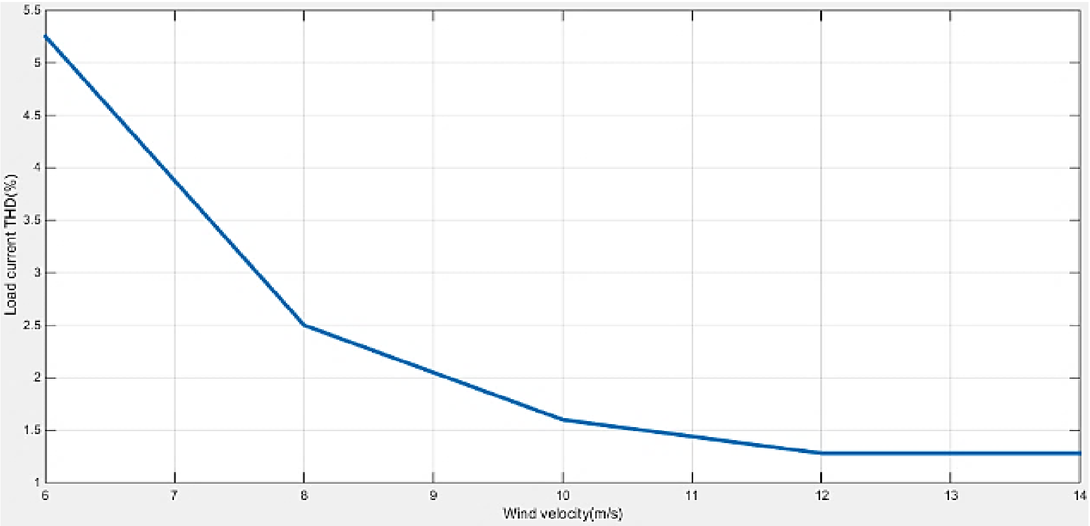

(a)

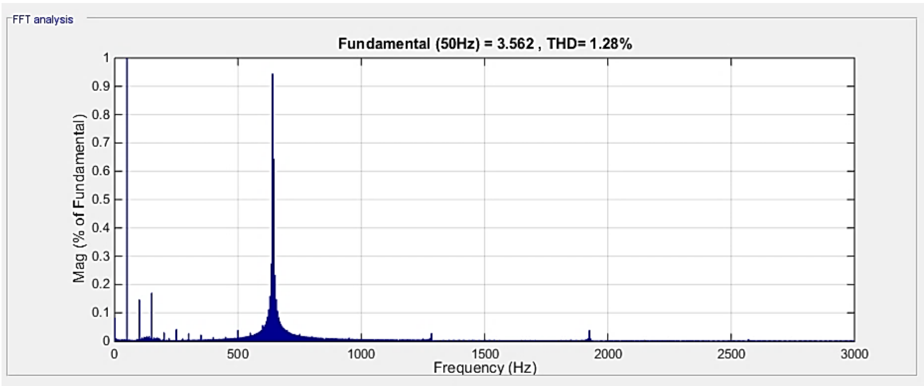

(b)

Figure 7. The variation of (a) the THD with wind velocity and (b) the spectrum of the load current (@12 m/s wind velocity)

5. CONCLUSION

This article proposed the control and management of a standalone wind power system against load and wind velocity variations. A simple MPPT algorithm is introduced to achieve high power utilization. The wind generator is connected to the load via a boost converter. It is utilized to implement the MPPT state using. The system dynamic model is derived then the control and energy management algorithms are introduced to improve the system performance. MATLAB simulations for the proposed standalone wind energy system were carried out. The system is tested under step variations of wind speed and load power. The simulation findings show the following. The proposed management system success to supply the loads perfectly under all disturbances. The performance of the load inverter controller is excellent, as the load power responses have small overshoots and small settling times. The DC-link voltage keeps tracking its reference perfectly. The AC load voltage and frequency are constants at their reference values. The load current THD with the proposed system is less than the standard value of 5%.

ACKNOWLEDGMENT

The authors extend their appreciation to the Deanship of Scientific Research of the University of Tabuk for funding this work through Research Group Grant number S-1441-0055.

APPENDIX

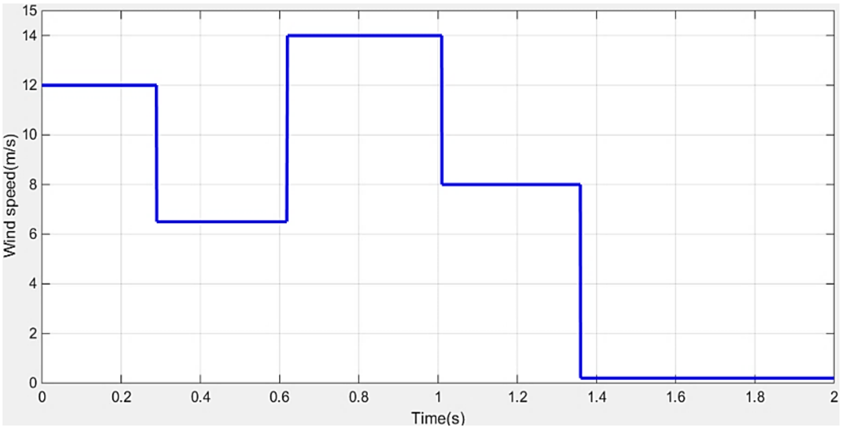

(a)

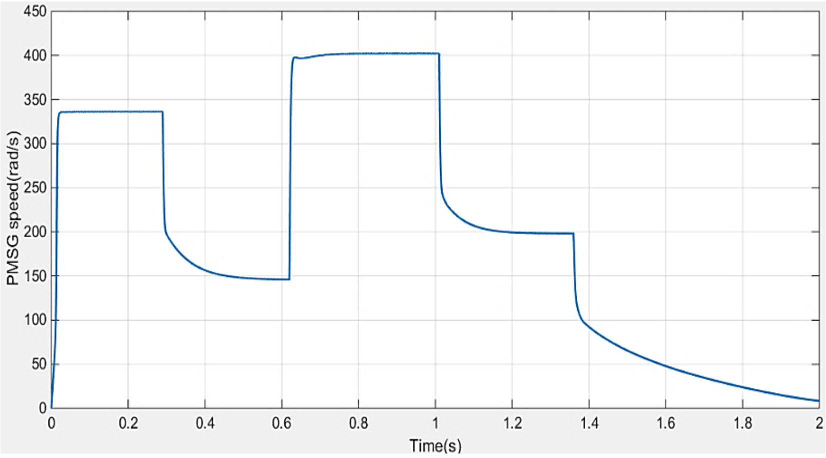

(b)

Figure 6. The proposed system results for the: (a) wind speed and (b) PMSG angular speed

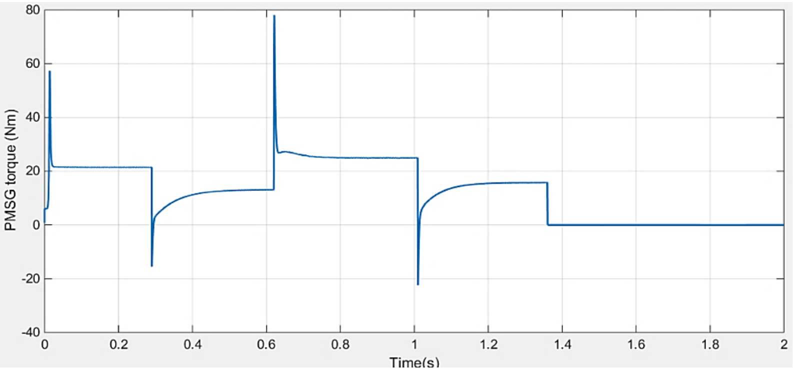

(c)

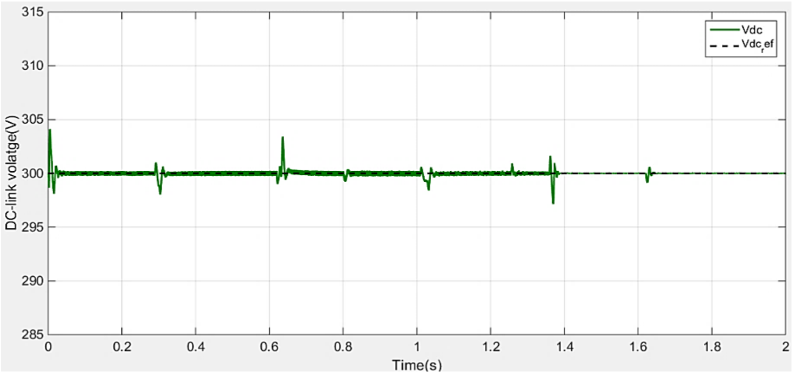

(d)

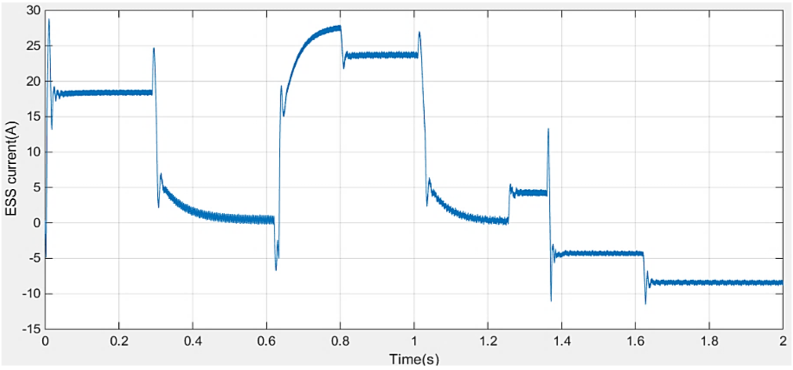

(e)

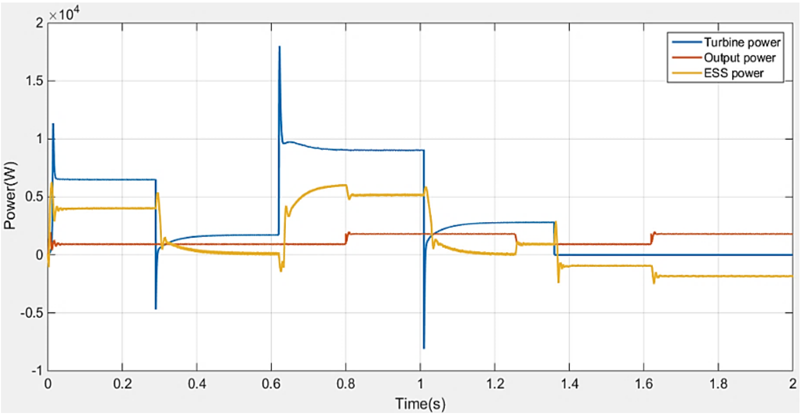

(f)

Figure 6. The proposed system results for the: (c) PMSG torque, (d) DC-link voltage, (e) energy storage current, and (f) system powers (continue)

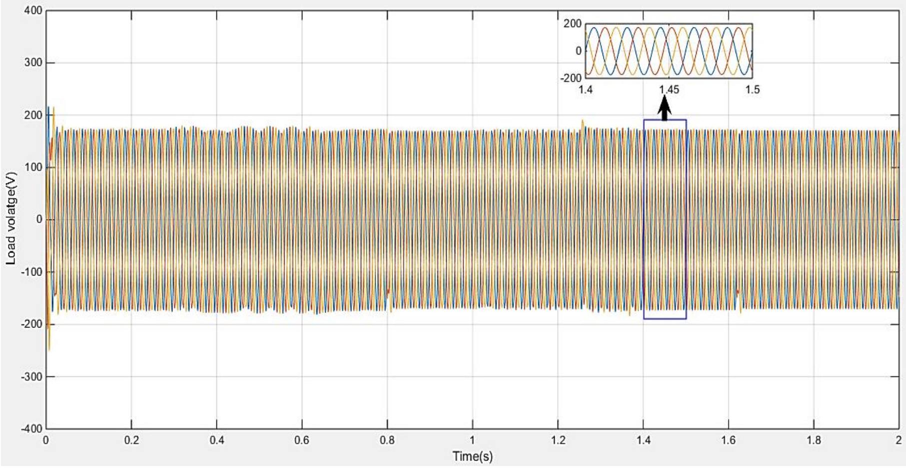

(g)

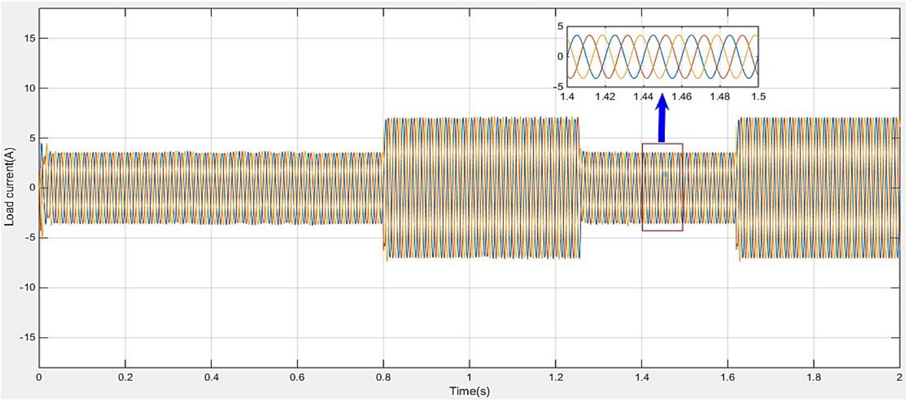

(h)

Figure 6. The proposed system results for the: (g) 3-φ load voltage and (h) 3-φ load current (continue)

REFERENCES

[1] I. E. Atawi, A. M. Kassem and S. A. Zaid, “Modeling, Management, and Control of an Autonomous Wind/Fuel Cell Micro-Grid System,” *Processes*, vol. *7*, no. 2, no. 1-22, 2019, doi: 10.3390/pr7020085.

[2] H. Azoug, H. Belmili and F. Bouazza, “Grid-connected control of PV-Wind hybrid energy system,” *International Journal of Power Electronics and Drive System*, vol. 12, no. 2, pp. 1228-1238, 2021, doi: 10.11591/ijpeds.v12.i2.pp1228-1238.

[3] B. I. Yassine and A. Boumediene, “Renewable energies evaluation and linking to smart grid,” *International Journal of Power Electronics and Drive System*, vol. 11, no. 1, pp. 107-118, 2020, doi: 10.11591/ijpeds.v11.i1.pp107-118.

[4] R. Rosso, X. Wang, M. Liserre, X. Lu and S. Engelken, “Grid-Forming Converters: Control Approaches, Grid-Synchronization, and Future Trends—A Review,” *IEEE Open Journal of Industry Applications*, vol. 2, pp. 93-109, 2021, doi: 10.1109/OJIA.2021.3074028.

[5] J. M. Guerrero, M. Chandorkar, T. Lee and P. C. Loh, “Advanced Control Architectures for Intelligent Microgrids—Part I: Decentralized and Hierarchical Control,” *IEEE Transactions on Industrial Electronics*, vol. 60, no. 4, pp. 1254-1262, 2013, doi: 10.1109/TIE.2012.2194969.

[6] A. Merabet, K. Tawfique Ahmed, H. Ibrahim, R. Beguenane and A. M. Y. M. Ghias, “Energy Management and Control System for Laboratory Scale Microgrid Based Wind-PV-Battery,” *IEEE Transactions on Sustainable Energy*, vol. 8, no. 1, pp. 145-154, 2017, doi: 10.1109/TSTE.2016.2587828.

[7] W. Wang, L. Liu, J. Liu and Z. Chen, “Energy management and optimization of vehicle-to-grid systems for wind power integration,” *CSEE Journal of Power and Energy Systems*, vol. 7, no. 1, pp. 172-180, 2021, doi: 10.17775/CSEEJPES.2020.01610.

[8] H. Bitaraf and S. Rahman, “Reducing Curtailed Wind Energy Through Energy Storage and Demand Response,” *IEEE Transactions on Sustainable Energy*, vol. 9, no. 1, pp. 228-236, 2018, doi: 10.1109/TSTE.2017.2724546.

[9] S. D. Ahmed, F. S. M. Al-Ismail, M. Shafiullah, F. A. Al-Sulaiman and I. M. El-Amin, “Grid Integration Challenges of Wind Energy: A Review,” *IEEE Access*, vol. 8, pp. 10857-10878, 2020, doi: 10.1109/ACCESS.2020.2964896.

[10] B. B. A. Amine, A. Ahmed and M. B. Houari, “Modeling, simulation and control of a doubly-fed induction generator for wind energy conversion systems,” *International Journal of Power Electronics and Drive System*, vol. 11, no. 3, pp. 1197-1210, doi: 10.11591/ijpeds.v11.i3.pp1197-1210.

[11] K. Noussi, A. Abouloifa, H. Katir, I. Lachkar, and F. Giri, “Nonlinear control of grid-connected wind energy conversion system without mechanical variables measurements,” *International Journal of Power Electronics and Drive Systems*, vol. 12, no. 2, pp. 1139-1149, 2021, doi: 10.11591/ijpeds.v12.i2.pp1139-1149.

[12] S. A. Zaid, *et al*., “Novel Fuzzy Controller for a Standalone Electric Vehicle Charging Station Supplied by Photovoltaic Energy,” *Applied System Innovation*, vol. 4, no. 3, pp. 1-13, 2021, doi: 10.3390/asi4030063.

[13] B. Amel, Z. Soraya, and C. Abdelkader, "Intelligent control of flywheel energy storage system associated with the wind generator for uninterrupted power supply," *International Journal of Power Electronics and Drive System*, vol. 11, no. 4, pp. 2062-2070, 2020, doi: 10.11591/ijpeds.v11.i4.pp2062-2072.

[14] V. Yaramasu, B. Wu, P. C. Sen, S. Kouro and M. Narimani, "High-power wind energy conversion systems: State-of-the-art and emerging technologies," *Proceedings of the IEEE*, vol. 103, no. 5, pp. 740-788, 2015, doi: 10.1109/JPROC.2014.2378692.

[15] H. Liu *et al*., "Subsynchronous Interaction Between Direct-Drive PMSG Based Wind Farms and Weak AC Networks," *IEEE Transactions on Power Systems*, vol. 32, no. 6, pp. 4708-4720, 2017, doi: 10.1109/TPWRS.2017.2682197.

[16] A. Harrouz, I. Colak and K. Kayisli, "Control of a small wind turbine system application," *IEEE International Conference on Renewable Energy Research and Applications (ICRERA)*, 2016, pp. 1128-1133, doi: 10.1109/ICRERA.2016.7884509.

[17] S. S. Saswat, S. Patra, D. P. Mishra, S. R. Salkuti and R. N. Senapati, "Harnessing wind and solar PV system to build hybrid power system," *International Journal of Power Electronics and Drive System*, vol. 12, no. 4, pp. 2160-2168, 2021, doi: 10.11591/ijpeds.v12.i4.pp2160-2168.

[18] I. E. Kararoui and M. Maaroufi, "Fuzzy sliding mode power control for wind power generation systems connected to the grid," *International Journal of Power Electronics and Drive System (IJPEDS)*, vol. 13, no. 1, pp. 606-619, 2022, doi: 10.11591/ijpeds.v13.i1.pp606-619.

[19] H. H. H. Mousa, A. R. Youssef, and E. E. Mohamed, "State of the art perturb and observe MPPT algorithms based wind energy conversion systems: A technology review," *International Journal of Electrical Power & Energy Systems*, vol. 126, pp. 106598, 2021, doi: 10.1016/j.ijepes.2020.106598.

[20] Y. Wang, Y. Yu, S. Cao, X. Zhang, and S. Gao, "A review of applications of artificial intelligent algorithms in wind farms," *Artificial Intelligence Review*, vol. 53, no. 5, pp. 3447-3500, 2020.

[21] M. N. Musarrat, M. R. Islam, K. M. Muttaqi and D. Sutanto, "Enhanced Frequency Support From a PMSG-Based Wind Energy Conversion System Integrated with a High Temperature SMES in Standalone Power Supply Systems," *IEEE Transactions on Applied Superconductivity*, vol. 29, no. 2, pp. 1-6, 2019, doi: 10.1109/TASC.2018.2882429.

[22] P. Anbarasan, M. Venmathi and V. Krishnakumar, "Modeling and Simulation of Standalone PMSG based Wind Energy Conversion System with Common Mode Voltage Suppression," *7th International Conference on Electrical Energy Systems (ICEES)*, 2021, pp. 85-88, doi: 10.1109/ICEES51510.2021.9383728.

[23] J. C. Y. Hui, A. Bakhshai and P. K. Jain, "An Energy Management Scheme with Power Limit Capability and an Adaptive Maximum Power Point Tracking for Small Standalone PMSG Wind Energy Systems," *IEEE Transactions on Power Electronics*, vol. 31, no. 7, pp. 4861-4875, 2016, doi: 10.1109/TPEL.2015.2478402.

[24] Y. Bai, B. Kou and C. C. Chan, "A Simple Structure Passive MPPT Standalone Wind Turbine Generator System," *IEEE Transactions on Magnetics*, vol. 51, no. 11, pp. 1-4, 2015, doi: 10.1109/TMAG.2015.2439043.

[25] H. Albalawi and S.A. Zaid, "Performance improvement of a grid-tied neutral-point-clamped 3-φ transformerless inverter using model predictive control," *Processes*, vol. 7, no. 11, pp. 1-17, 2019, doi: 10.3390/pr7110856.

[26] A. Kusumawardana, L. Gumilar, D. Prihanto, H. Wicaksono, S. N. T. Saputra and D. Prasetyo, "Simple MPPT based on Maximum Power with Double Integral Sliding Mode Current Control for Vertical Axis Wind Turbine," *IEEE Conference on Energy Conversion (CENCON)*, 2019, pp. 31-36, doi: 10.1109/CENCON47160.2019.8974725.

[27] P. Huynh, S. Tungare and A. Banerjee, "Maximum Power Point Tracking for Wind Turbine Using Integrated Generator–Rectifier Systems," *IEEE Transactions on Power Electronics*, vol. 36, no. 1, pp. 504-512, 2021, doi: 10.1109/TPEL.2020.3002254.

BIOGRAPHIES OF AUTHORS

Hani Albalawi received his B.Sc. degree in electrical engineering from King Abdulaziz University, Jeddah, Saudi Arabia, in 2008, the M.S. degree in automatic control system engineering from the University of Sheffield, Sheffield, UK, in 2011 and the Ph.D. degree from Clemson University, Clemson, SC, USA in 2016. He is a Faculty Member at the Department of Electrical Engineering, Faculty of Engineering and Director of Renewable Energy and Energy Efficiency (REEEC) Center at the University of Tabuk, Saudi Arabia. His research interests include renewable energy, energy management, energy storage, power system quality, power system planning and operation, and power system control. He can be contacted at email: halbala@ut.edu.sa.

Sherif A. Zaid was born in Cairo, Egypt 1970. Received BSC 1992, MSC 1996, and Ph.D. 2001 in electrical engineering from faculty of engineering, Cairo University, Giza, Egypt. Now, he is a full professor of power electronics at Cairo University, Faculty of Engineering, Department of Electrical power. His research interests are power electronics, renewable energy systems, and electrical drives. He has published around sixty research papers and participated in many research projects. Also, he is a reviewer for many reputable journals. He can be contacted at email: shfaraj@ut.edu.sa.

.

Yonis M. Buswig received his B.Eng. degree from Omar Al-Mukhtar University, Libya, in 2008. The M.Sc. degree in electrical and electronics engineering from Tun Hussein Onn University of Malaysia (UTHM), Batu Pahat, Johor, Malaysia, in 2011. In 2015, he was awarded his Ph.D. degree from Department of Power Engineering, Faculty of Electrical Engineering, Tun Hussein Onn University of Malaysia (UTHM). Currently, He is a Lecturer in the Electrical and Electronic Engineering Department, Faculty of Engineering, Universiti Malaysia Sarawak. His current research interests include the area of Power Electronics, Renewable energy technology, and Motor Drives Control. He can be contacted at email: byonis@unimas.my.

Hassan Wedaa El-Rab was born in Qena, Egypt in 1976. He received the BSc, MSc, PhD degrees in electrical engineering from Assiut University, Egypt, in 1999, 2004, and 2012, respectively. From 2008 to 2010, he was with the department of Environmental and Life Sciences, Toyohashi University of Technology, Toyohashi, Japan as a researcher. From 2012 to 2015, he became an assistant professor at the Electrical Engineering Department, Assiut University From 2015 until now, he was with the Electrical Engineering Department, University of Tabuk, Saudi Arabia as an assistant professor. His research activities include digital calculation of electric fields, partial-discharge analysis, and assessment in electric power equipments, and simulation and modeling of the high voltage phenomena. He can be contacted at email: habdaldaiem@ut.edu.sa.

Abderrahim Lakhouit was born in Morocoo in 1976, He is an associate professor in environmental engineering at Tabuk University, his research interest is in civil engineering, environmental engineering, water, air pollution, and waste management. He can be contacted at email: a.lakhouit@ut.edu.sa.

Muhammed Ayaz Arshad received the M.S. degree in computer science with specialization in computer networks and wireless communication from the Shaheed Zulfikar Ali Bhutto Institute of Science and Technology, Islamabad, Pakistan, and the Ph.D. degree in information technology from Universiti Teknologi Petronas, Malaysia, in 2007 and 2011, respectively. He was an Assistant Professor with the Computer Science Department, Federal Urdu University of Arts Science and Technology, Islamabad, Pakistan from 2007 to 2008. His research interests include mobile and sensor networks, routing protocols, network security, and underwater acoustic sensor networks. He is the author of many research articles published under leading journals. He is currently an Assistant Professor and a member of Sensor Networks and Cellular Systems Research Center, University of Tabuk, Saudi Arabia. He can be contacted at email: Miyaz@ut.edu.sa.